Role of Phase Variables in Quarter-Filled Spin Density Wave States*

Yuh TOMIO[1], and Yoshikazu SUZUMURA[1,2]

[1] *Department of Physics, Nagoya University, Nagoya 464-8602*
[2] *CREST, Japan Science and Technology Corporation (JST)*

(Received November 1, 1999)

Several kinds of spin density wave (SDW) states with both quarter-filled band and dimerization are reexamined for a one-dimensional system with on-site, nearest-neighbor and next-nearest-neighbor repulsive interactions, which has been investigated by Kobayashi *et al.* (J. Phys. Soc. Jpn **67** (1998) 1098). Within the mean-field theory, the ground state and the response to the density variation are calculated in terms of phase variables, θ and ϕ, where θ expresses the charge fluctuation of SDW and ϕ describes the relative motion between density wave with up spin and that with down spin respectively. It is shown that the exotic state of coexistence of $2k_{\rm F}$-SDW and $2k_{\rm F}$-charge density wave (CDW) is followed by $4k_{\rm F}$-SDW but not by $4k_{\rm F}$-CDW where $k_{\rm F}$ denotes a Fermi wave vector. The harmonic potential with respect to the variation of θ and/or ϕ disappears for the interactions, which lead to the boundary between the pure $2k_{\rm F}$-SDW state and the corresponding coexistent state.

KEYWORDS: spin density wave, quarter-filled band, charge density, phase variable, long range Coulomb interaction

§1. Introduction

Spin density wave (SDW) state has been studied extensively for quasi-one-dimensional organic conductors, $(TMTSF)_2X$ and $(TMTTF)_2X$, which are known as Bechgaard salt.[1,2] Since the energy band of the salt is anisotropic and quarter-filled, the SDW state is determined essentially by the nesting along the one-dimensional direction where the corresponding Fermi wave vector, $k_{\rm F}$, is $k_{\rm F} = \pi/4$ in the unit of lattice constant. The ground state of such a SDW, which has been studied by NMR experiment,[3,4] exhibits the periodic array of magnetic moment along the one-dimensional axis where the periodicity is four times as large as the lattice constant and the magnitude varies every two lattice sites. The degree of dimerization, which reduces the system effectively to the half-filled one, has been estimated in these salt.[5] Another noticeable feature of this SDW state is the charge fluctuation, which is caused by the deformation of the phase of the density wave, as seen in the nonlinear electric conductivity.[6]

Recently the X-ray scattering investigation has shown that $2k_{\rm F}$-SDW coexists with $2k_{\rm F}$-charge density wave (CDW) in the SDW state of $(TMTSF)_2PF_6$ at temperatures just below the onset temperature of the SDW ordering.[7] The $4k_{\rm F}$ satellite reflection is also observed for both $(TMTSF)_2PF_6$ and $(TMTTF)_2Br$. Further the coexistent state of $2k_{\rm F}$-SDW, $2k_{\rm F}$-CDW and $4k_{\rm F}$-CDW has been verified in the temperature range 4-12 K corresponding to SDW1 phase while CDW is absent in SDW3 phases at lower temperatures.[8]

Theoretical study for the coexistence of SDW and CDW has been explored based on the mean-field theory. Seo and Fukuyama[9] have found the coexistence of $2k_{\rm F}$-SDW and $4k_{\rm F}$-CDW by examining the extended Hubbard model, which takes into account both nearest-neighbor repulsive interaction and dimerization. The SDW state, which is followed by $4k_{\rm F}$-CDW, appears when the magnitude of nearest-neighbor interaction is larger than a critical value. Based on this model, the collective mode describing the charge fluctuation was calculated. The excitation spectrum, which has a gap due to commensurability, becomes gapless for the nearest-neighbor interaction leading to the onset of the coexistence.[10] The noticeable state of the coexistence of $2k_{\rm F}$-SDW and $2k_{\rm F}$-CDW has been demonstrated by Kobayashi *et al.* who introduced the next-nearest-neighbor interaction.[11] They examined the SDW state as the function of both the nearest-neighbor interaction (V_a) and the next-nearest-neighbor interaction (V_2) and found the phase diagram, in which such a coexistent state is located in the region with large V_a and large V_2. Thus the model with the long range Coulomb interaction reveals the ground state with variety of SDW states. However it is not yet clear if $4k_{\rm F}$-SDW state and/or $4k_{\rm F}$-CDW state can coexist in addition to the $2k_{\rm F}$-CDW.

In the present paper, such a calculation is performed for a model proposed by Kobayashi *et al.*,[11] within the mean-field theory. The ground state is examined in terms of two kinds of phase variables θ and ϕ, where θ is a phase of $2k_{\rm F}$-SDW and ϕ is the difference between a phase of density wave with up spin and that with down spin. Further, as a first step for studying the density fluctuation, we examine the increase of energy, which is caused by varying these two kinds of phases from those of the ground state. In §2, formulation is given for the model, which comprises dimerization and alternating transfer energy (t_a and t_b) with repulsive interaction (U), the alternating nearest-neighbor interaction (V_a and V_b) with the fixed V_b/V_a and the next-nearest-neighbor interac-

* to be published in J. Phys. Soc. Jpn. **69** No.3 (2000) 796

tion (V_2). The order parameters is examined in terms of phase variable θ and ϕ. In §3, the ground state of the SDW is calculated to obtain a phase diagram on the plane of V_2/V_a and V_a/t_b. Based on the study of the ground state, the property of the density variation is investigated by calculating the energy as a function of θ and ϕ. Discussion is given in §4.

§2. Formulation

We study the SDW state with the quarter-filled band by use of a one-dimensional extended Hubbard model with dimerization and long range Coulomb interaction. The model is represented as

$$H = -\sum_{\sigma=\uparrow,\downarrow}\sum_{j=1}^{N}\left(t-(-1)^j t_{\rm d}\right)\left(C_{j\sigma}^{\dagger}C_{j+1,\sigma}+{\rm h.c.}\right) + H_{\rm int} \ , \tag{2.1}$$

$$H_{\rm int} = U\sum_{j=1}^{N} n_{j\uparrow}n_{j\downarrow} + \sum_{j=1}^{N}\left(V-(-1)^j\delta V\right)n_j n_{j+1} + V_2\sum_{j=1}^{N} n_j n_{j+2} \ , \tag{2.2}$$

where $t_a = t + t_{\rm d}$, $t_b = t - t_{\rm d}$, $V_a = V + \delta V$ and $V_b = V - \delta V$. The quantity $C_{j\sigma}^{\dagger}$ ($C_{j\sigma}$) denotes the creation (annihilation) operator of the electron at the j-th lattice site with spin σ. The quantity N is the total number of the lattice site. $n_{j\sigma} = C_{j\sigma}^{\dagger}C_{j\sigma}$ and $n_j = n_{j\uparrow} + n_{j\downarrow}$. We take t, $k_{\rm B}$ and the lattice constant as unity. The alternation of the transfer integrals given by $t \pm t_{\rm d}$ comes from dimerization, which induces the energy, $t_{\rm d}$. Coupling constants for the Coulomb interaction are defined by U, $V \pm \delta V$ and V_2, which denote the on-site repulsive interaction, the nearest-neighbor interaction and the next-nearest-neighbor interaction, respectively. The quantity δV also originates in the dimerization. By noting that the electron band is at quarter-filling, order parameters of density wave can be written as ($m = 0, 1, 2, 3$),

$$S_{mQ_0} = \frac{1}{N}\sum_{\sigma=\uparrow,\downarrow}\sum_{-\pi<k\le\pi}{\rm sgn}(\sigma)\left\langle C_{k\sigma}^{\dagger}C_{k+mQ_0,\sigma}\right\rangle_{\rm MF} \ , \tag{2.3a}$$

$$D_{mQ_0} = \frac{1}{N}\sum_{\sigma=\uparrow,\downarrow}\sum_{-\pi<k\le\pi}\left\langle C_{k\sigma}^{\dagger}C_{k+mQ_0,\sigma}\right\rangle_{\rm MF} \ , \tag{2.3b}$$

where $Q_0 \equiv 2k_{\rm F} = \pi/2$ with $k_{\rm F}$ being the Fermi wave vector. The spatial dependence of electron densities with up and down spin, which has the periodicity being four times as large as the lattice constant, is obtained from the Fourier transform of eqs. (2.3a) and (2.3b). Then we examine eqs. (2.3a) and (2.3b) under the condition that $S_0 = 0$, $D_0 = 1/2$, $S_{Q_0} = S_{3Q_0}^{*}$, $D_{Q_0} = D_{3Q_0}^{*}$, $S_{2Q_0} = S_{2Q_0}^{*} \equiv S_2$ and $D_{2Q_0} = D_{2Q_0}^{*} \equiv D_2$. In terms of the mean-field (MF) given by eqs. (2.3a) and (2.3b), Hamiltonian (eq. (2.1)) is expressed as

$$\begin{aligned} H_{\rm MF} = \sum_{\sigma=\uparrow,\downarrow}\sum_{-\pi<k\le\pi}\Bigg[&\left(\varepsilon_k + \frac{U}{4} + V + V_2\right)C_{k\sigma}^{\dagger}C_{k\sigma} \\ &+\Bigg\{\Big((\frac{U}{2}-2V_2)D_{Q_0} + 2{\rm i}\delta V D_{Q_0}^{*} - {\rm sgn}(\sigma)\frac{U}{2}S_{Q_0}\Big) \\ &\times C_{k+Q_0,\sigma}^{\dagger}C_{k\sigma} + {\rm h.c.}\Bigg\} \\ &+\Big((\frac{U}{2}-2V+2V_2)D_{2Q_0} - {\rm sgn}(\sigma)\frac{U}{2}S_{2Q_0} \\ &- 2{\rm i}t_{\rm d}\sin k\Big)C_{k\sigma}^{\dagger}C_{k+2Q_0,\sigma}\Bigg] \\ &+NU\left[-\frac{1}{16} - \frac{1}{2}\left(|D_{Q_0}|^2 - |S_{Q_0}|^2\right) - \frac{1}{4}\left(D_{2Q_0}^2 - S_{2Q_0}^2\right)\right] \\ &+NV\left(-\frac{1}{4} + D_{2Q_0}^2\right) + {\rm i}N\delta V\left(D_{Q_0}^2 - D_{Q_0}^{*2}\right) \\ &+NV_2\left(-\frac{1}{4} + 2|D_{Q_0}|^2 - D_{2Q_0}^2\right) \ , \end{aligned} \tag{2.4}$$

where $\varepsilon_k = -2t\cos k$. Since the nesting vector is given by $Q_0 = \pi/2$, the eigenvalue of eq. (2.4) exhibits four energy bands $E_{\rm n}(k)$, (n $= 1, 2, 3, 4$), where $E_1(k) < E_2(k) < E_3(k) < E_4(k)$. In the ground state, the lowest energy band, $E_1(k)$, is fully occupied and others are empty due to the quarter-filling. By solving eqs. (2.3a) and (2.3b) self-consistently, the ground state energy per site, $E_{\rm g}$, is obtained as

$$\begin{aligned} E_{\rm g} = &\frac{1}{N}\sum_{\sigma}\sum_{0<k\le Q_0}E_1(k) \\ &+U\left[-\frac{1}{16} - \frac{1}{2}\left(|D_{Q_0}|^2 - |S_{Q_0}|^2\right) - \frac{1}{4}\left(D_{2Q_0}^2 - S_{2Q_0}^2\right)\right] \\ &+V\left(-\frac{1}{4} + D_{2Q_0}^2\right) + {\rm i}\delta V\left(D_{Q_0}^2 - D_{Q_0}^{*2}\right) \\ &+V_2\left(-\frac{1}{4} + 2|D_{Q_0}|^2 - D_{2Q_0}^2\right) \ , \end{aligned} \tag{2.5}$$

where the Brillouin zone is reduced to $0 < k \le Q_0$. In terms of eq. (2.5), we define the quantity, δE, as

$$\delta E = E_{\rm g} - E_{\rm normal} \ , \tag{2.6}$$

which denotes the difference between the ground state energy of the ordered state and that of the normal state i.e., $S_j = D_j = 0$ ($j = 1, 2$). In eq. (2.6), $E_{\rm normal}$ ($= -2\sqrt{2}t/\pi + U/16 + V/4 + V_2/4$) is the energy of the normal state.

Now we examine the SDW state from the aspect of the phase variable. Since $S_{Q_0} = S_{3Q_0}^{*}$ and $D_{Q_0} = D_{3Q_0}^{*}$, eqs. (2.3a) and (2.3b) are expressed as

$$S_{Q_0} = S_1{\rm e}^{{\rm i}\theta} \ , \tag{2.7a}$$

$$D_{Q_0} = D_1{\rm e}^{{\rm i}\theta'} \ , \tag{2.7b}$$

where $S_1 (> 0)$ and $D_1 (> 0)$ are real. Quantities θ and θ' are phase factors. Within the present numerical calculation, we find always $S_{Q_0}/S_1 = {\rm i}D_{Q_0}/D_1$ for the ground state. Thus we calculate the energy under such

a restriction, i.e., eq. (2.7b) is replaced by

$$D_{Q_0} = D_1 \mathrm{e}^{\mathrm{i}(\theta-\pi/2)} \ . \tag{2.8}$$

In terms of eqs. (2.3a), (2.3b), (2.7a) and (2.8), the electron density for spin σ at the j-th site is expressed as

$$\langle n_{j\sigma}\rangle = 1/4 + \mathrm{sgn}(\sigma) S_1 \cos(Q_0 r_j + \theta) + D_1 \sin(Q_0 r_j + \theta) + \frac{1}{2}\left(D_2 + \mathrm{sgn}(\sigma) S_2\right)\cos(2Q_0 r_j) \ . \tag{2.9}$$

The respective electron density is rewritten as

$$\langle n_{j\uparrow}\rangle = 1/4 + A\sin(Q_0 r_j + \theta + \phi) + B\cos(2Q_0 r_j) \ , \tag{2.10a}$$

$$\langle n_{j\downarrow}\rangle = 1/4 + A\sin(Q_0 r_j + \theta - \phi) + C\cos(2Q_0 r_j) \ , \tag{2.10b}$$

where $A = \sqrt{S_1^2 + D_1^2}$, $\phi = \tan^{-1}(S_1/D_1)$, $B = (D_2+S_2)/2$ and $C = (D_2-S_2)/2$. Equations (2.10a) and (2.10b) imply that the density wave with up (down) spin has a phase $\theta + \phi$ ($\theta - \phi$). The quantity, ϕ, expresses the relative motion between the density wave with up spin and that with the down spin. The idea, that $\phi \neq 0$ leads to the coexistence of $2k_{\mathrm{F}}$-SDW and $2k_{\mathrm{F}}$-CDW, has been already asserted by Overhauser.[12] The quantity, θ, denotes a phase representing the charge density fluctuation, which gives rise to the sliding motion of the SDW.[13, 14, 15, 16, 17]

The calculation of the energy can be implemented by two kinds of methods, i.e., parameters determined self-consistently are given either by S_1, S_2, D_1, D_2 and θ or by A, S_2, D_2, θ and ϕ. For the simplicity, the former choice is taken for the calculation of the ground state while the latter one is used for studying the effect of the variation of phases θ and ϕ around the ground state. We define $\tilde{V}$ as the energy in the presence of density waves with S_{nQ_0} and D_{nQ_0} (n=1,2 and 3), which are introduced as the trial function. From eqs. (2.4), (2.7a) and (2.8) together with $\phi = \tan^{-1}(S_1/D_1)$, $\tilde{V}$ is written as

$$\tilde{V} \equiv \frac{1}{N}\langle H_{\mathrm{MF}}\rangle - \frac{U}{16} - \frac{V}{4} - \frac{V_2}{4} \ . \tag{2.11}$$

The average, $\langle\ \rangle$, is performed by eq. (2.4), in which quantities S_{nQ_0} and D_{nQ_0} are retained as parameters. Note that eqs. (2.3a) and (2.3b) are equivalent to the condition that

$$\frac{\partial\tilde{V}}{\partial S_j} = \frac{\partial\tilde{V}}{\partial D_j} = 0 \ , \qquad (j = 1, 2) \ , \tag{2.12}$$

$$\frac{\partial\tilde{V}}{\partial\theta} = 0 \ , \tag{2.13}$$

and $N^{-1}\sum_j \langle n_{j\sigma}\rangle = 1/4$. Then we introduce a quantity, $V(\theta,\phi)$, which is defined by

$$V(\theta,\phi) \equiv \tilde{V}\big|_{\frac{\partial\tilde{V}}{\partial A}=\frac{\partial\tilde{V}}{\partial S_2}=\frac{\partial\tilde{V}}{\partial D_2}=0} \ . \tag{2.14}$$

The minimum of $V(\theta,\phi)$ is given by $\theta = \theta_0$ and $\phi = \phi_0$, i.e., quantities θ_0 and ϕ_0 are phases for the ground state. Thus, we can evaluate the increase of energy by $V(\theta,\phi)$ when the phase variables are varied from the ground state. Especially the limiting behavior for small variation of these phases is evaluated by expanding $V(\theta,\phi)$ in terms of $\theta - \theta_0 (\equiv r\cos\psi)$ and $\phi - \phi_0 (\equiv r\sin\psi)$. For $r \ll 1$, one obtains

$$V(\theta,\phi) = V(\theta_0,\phi_0) + C(\psi) r^2 + \cdots \ , \tag{2.15}$$

where $C(\psi)$ denotes the coefficient of harmonic potential.

§3. SDW States and Phase Variables

3.1 Ground state

We examine the possible ground state, which gives the lowest energy in the solution of the self-consistency equations. From the numerical calculation, we found three kinds of solutions for SDW states shown in Fig. 1: pure 2-k_{F}-SDW (I), a coexistent state of $2k_{\mathrm{F}}$-SDW and $4k_{\mathrm{F}}$-CDW (II) and that of $2k_{\mathrm{F}}$-SDW, $2k_{\mathrm{F}}$-CDW and $4k_{\mathrm{F}}$-SDW (III). The pure 2-k_{F}-SDW state is obtained for the interaction of only U.[17] A coexistent state of $2k_{\mathrm{F}}$-SDW and $4k_{\mathrm{F}}$-CDW[9] appears for V lager than a critical value. An exotic state of the coexistence of $2k_{\mathrm{F}}$-SDW and $2k_{\mathrm{F}}$-CDW has been obtained for large V and large V_2.[11] This state differs from the state III in the sense that $4k_{\mathrm{F}}$-SDW also coexists in the state III. It seems to be reasonable that the state III could be possible if the order parameter for $4k_{\mathrm{F}}$-SDW is treated in a perturbational method .

In the present calculation, we examine self-consistency equations by varying V_a/t_b and V_2/V_a. Parameters are chosen as $t_a/t_b = 1.1$, $V_b/V_a = 0.8$ and $U/t_b = 4$,[11] where the magnitude of dimerization seems to be reasonable for the Bechgaard salts.[5] Figure 2(a) displays the V_a/t_b-dependence of S_1, S_2 and D_1, which denote amplitudes for $2k_{\mathrm{F}}$-SDW, $4k_{\mathrm{F}}$-SDW and $2k_{\mathrm{F}}$-CDW re-

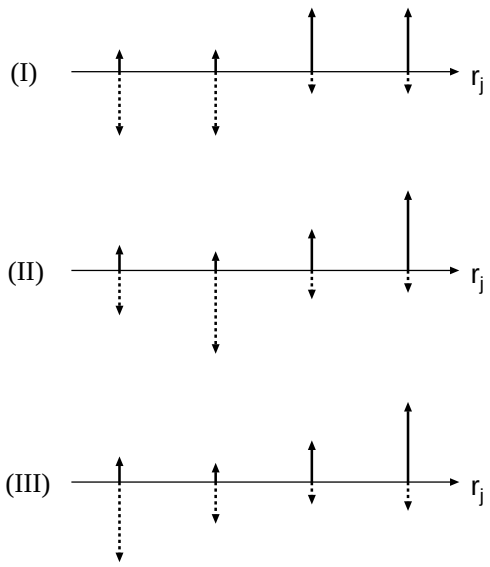

Fig. 1. The electron density $< n_{j\sigma} >$ as the function of the lattice site r_j for three kinds of SDW states: pure 2-k_{F}-SDW (I), a coexistence of $2k_{\mathrm{F}}$-SDW and $4k_{\mathrm{F}}$-CDW (II) and a coexistence of $2k_{\mathrm{F}}$-SDW, $2k_{\mathrm{F}}$-CDW and $4k_{\mathrm{F}}$-SDW (III). The variation satisfies $< n_{j+4} >=< n_j >$ where the solid (dashed) arrow denotes the magnitude of electron density with up (down) spin.

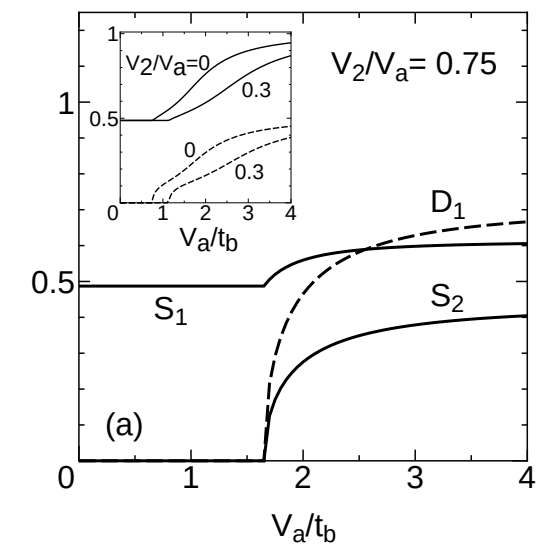

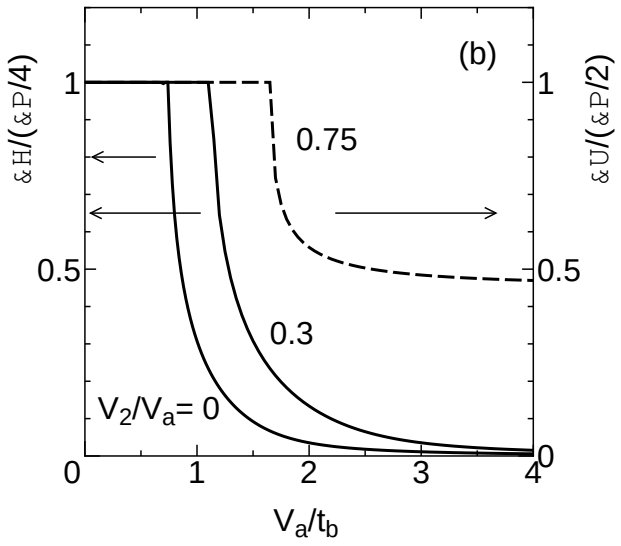

Fig. 2. (a) The V_a/t_b-dependence of order parameters S_1, S_2 and D_1 for $V_2/V_a = 0.75$. In the inset, order parameters, S_1 (solid curve) and D_2 (dashed curve) are shown for $V_2/V_a = 0$ and 0.3. Order parameters are zero if not shown explicitly. (b) The V_a/t_b-dependence of θ (solid curve) for $V_2/t_b = 0$ and 0.3 and that of ϕ (dashed curve) for $V_2/t_b = 0.75$.

spectively . For $V_2/V_a = 0.75$, the state I moves to the state III at $V_a/t_b = 1.66$, where both D_1 and S_2 starts increasing continuously with a slight enhancement of S_1. Such a simultaneous appearance of D_1 and S_2 originates in the fact that the term proportional to $D_1S_2S_1$ exists in the expansion of the Ginzburg-Landau free energy. Note that $D_2 = 0$, i.e., $4k_{\rm F}$-CDW is absent for $V_2/V_a = 0.75$. In the inset, the V_a/t_b-dependence of order parameters for $V_2/V_a = 0$ and 0.3 is shown where solid curve and dashed curve denote S_1 and D_2 respectively. The transition from the state I into the state II takes place at $V_a/t_b = 0.76$ and 1.13 for $V_2/V_a = 0$ and 0.3 respectively where $S_2 = D_1 = 0$ for any V_a/t_b. It is found that S_1 in the state I does not depend on both V_a and

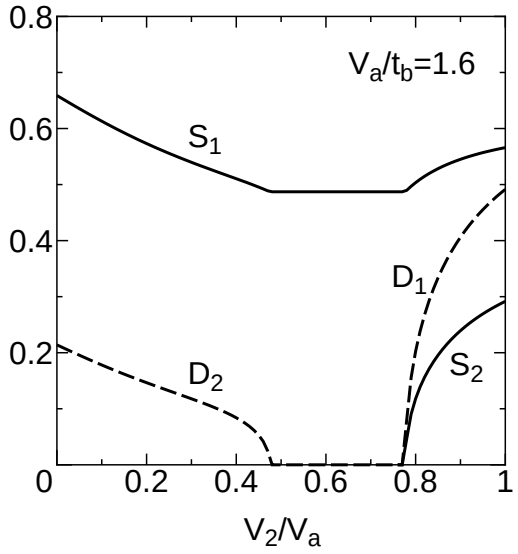

Fig. 3. The V_2/V_a-dependence of order parameters, S_1, S_2, D_1 and D_2, for V_a/t_b =1.6.

V_2 and that the state II is followed by $4k_{\rm F}$-CDW. In Fig. 2(b), quantity θ corresponding to $V_2/t_b = 0$ and 0.3 is shown by the solid curve. When the state I moves to the state II, θ decreases rapidly from $\pi/4$ and ϕ remains at $\phi = \pi/2$ for both states. The dashed curve denotes ϕ for $V_2/t_b = 0.75$, which shows a transition from the state I into the state III. The quantity ϕ decreases from $\pi/2$ while $\theta = \pi/4$ for both states I and III. Note that the coexistence of $2k_{\rm F}$-SDW and $2k_{\rm F}$-CDW in the state III originates in ϕ with $0 < \phi < \pi/2$.

Figure 3 shows the successive transition from the state II, the state I and the state III with increasing V_2/V_a. Order parameters S_1, S_2, D_1 and D_2 are shown as a function of V_2/V_a with the fixed V_2/t_b =1.6. A transition from the state II into state I occurs at $V_2/V_a = 0.48$ while a transition from the state I into state III occurs at V_2/V_a = 0.78. The V_2-dependence of D_2, D_1 and S_2 indicates the transition being of the second order. The quantities D_1 and S_2 appear at the same V_2/V_a, as seen in Fig. 2. A linear dependence of the variation of S_1, which is found just below the transition at $V_2/V_a = 0.48$, comes from the effect of higher order with respect to D_2. In the state I, S_1 does not depend on V_2 since the pure $2k_{\rm F}$-SDW is determined only by the U-term, i.e., the density-density interaction of both $V \pm \delta V$-term and V_2-term does not give rise to the coupling between the order parameter of pure $2k_{\rm F}$-SDW and others. The appearance of D_1 and D_2 is understood as follows. The distance for the next-nearest-neighbor interaction, V_2, corresponds to the $2k_{\rm F}$-periodicity. Then the $2k_{\rm F}$-CDW is induced for V_2 larger than a critical value, *e.g.*, D_1 appears for $V_2/t \gtrsim 1.3$ and irrespective of the magnitude of V. In a similar way, one can understand the role of the nearest-neighbor interaction, V, which induces D_2 for large V_a (or V) due to the $4k_{\rm F}$-periodicity. The interval region in Fig. 3 corresponding to the state I decreases with increasing V and disappears for V (and/or $V_a(= V + \delta V)$) larger than a

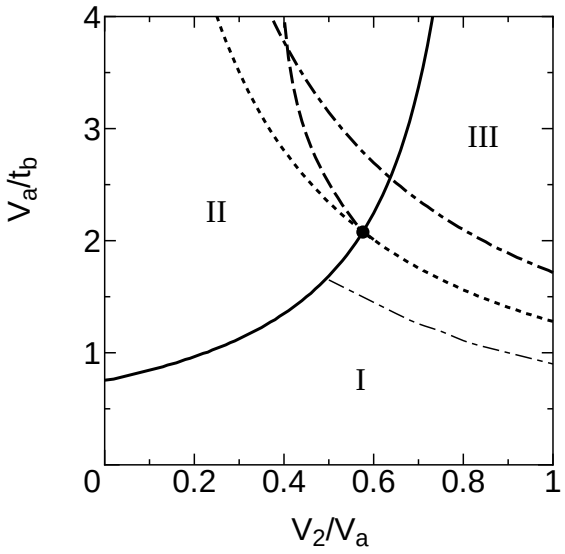

Fig. 4. Phase diagram on the plane of V_2/V_a and V_a/t_b with $t_a/t_b = 1.1$, $V_b/V_a = 0.8$ and $U/t_b = 4$. The closed circle given by $(V_2, V_a) = (V_{2,c}, V_{a,c})$ denotes an intersection of the solid curve and the dotted curve. The solid curve (dotted curve), which shows the boundary between the region I and the region II (the region I and the region III) becomes the actual boundary for $V_a < V_{a,c}$. The boundary between the state II and the state III is given by the dashed curve. The thick dash-dotted curve corresponds to the dotted curve with $S_2 = 0$[11] and the thin dash-dotted curve is explained in the inset of Fig. 7(b).

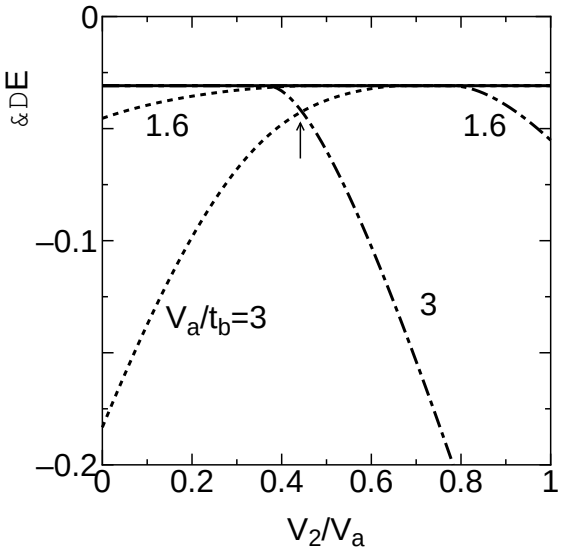

Fig. 5. The V_2/V_a-dependence of energy δE (eq. (2.6)) with the fixed $V_a/t_b = 1.6$ and 3, for the state I (solid curve), the state II (dotted curve) and the state III (dash-dotted curve).

critical value.

In Fig. 4, a phase diagram of SDW states is shown on the plane of V_2/V_a and V_a/t_b for $U/t_b = 4$, which is equal to U/t= 3.81. The closed circle corresponding to the intersection of the solid curve and the dotted curve denotes a critical point given by $(V_{2,c}/V_a, V_{a,c}/t_b)(\simeq (0.576, 2.077)$, at which all the energies of states I, II and III become equal. The solid curve (the dotted curve) shows the boundary between the sate I and the state II (the state I and the state III). The dashed curve is the boundary between the state II and the state III. On the dashed curve, the energy of the state II becomes equal to that of the state III, while amplitudes of both order parameters are finite. For $V_a < V_{a,c}$, the second order transition occurs on both the solid curve and the dotted curve while the first order transition from the state II into the state III is obtained on the dashed curve. We note that the state III with the assumption of $S_2 = 0$ has been already obtained[11] where the resultant boundary between the state I and the state III is shown by the thick dash-dotted curve in Fig. 4. Compared with the present boundary of the dotted curve, the region for the state III is suppressed in the absence of S_2. The thin dash-dotted curve, which is not a boundary, is explained in the discussion of the inset of Fig. 7(b).

The first order transition shown by the dashed curve of Fig. 4 is examined by calculating the energy gain in the ordered state, δE, which is defined by eq. (2.6). In Fig. 5, the V_2/V_a-dependence of δE is shown for $V_a/t_b =$ 1.6 and 3. The solid curve, the dotted curve and the dash-dotted curve denote δE for the state I, II and III respectively. The quantity δE for the state I, which is independent of the magnitude of V_a/t_b, is largest compared with those of the state II and the state III. The case of $V_a/t_b = 1.6$ corresponds to Fig. 3, which shows a successive transition given by the state II, the state I and the state III with increasing V_2/V_a. For $V_a/t_b = 3$, one obtains a first order transition from the state II into the state III at $V_2/V_a = 0.45$, which is shown by the arrow. Based on these calculations,we find the V_2/V_a and V_a/t_b dependences of δE in Fig. 4 as follows. The quantity δE in the region I does not depend on both V_2/V_a and V_a/t_b while δE in region II (III) decreases motonically with moving away from the boundary of the solid curve (the dotted curve).

3.2 Property around the ground state

In the previous section, the ground sate has been studied by calculating order parameters where their phases $\theta(\rightarrow \theta_0)$ and $\phi(\rightarrow \phi_0)$ are also determined so as to minimize the energy. We examine, in this section, the property around the ground state by calculating $V(\theta, \phi)$ given by eq. (2.14) which denotes the energy obtained by the phase variation. The study is focused on the state around the boundary given by the solid curve and the dotted curve in Fig. 4.

Figure 6(a) shows the θ-dependence of $V(\theta, \pi/2)$ for three cases which are located close to the boundary of the solid curve of Fig. 4. Solid curve, dotted curve and dash-dotted curve are calculated for $V_a/t_b = 0.5$ (1), 1.13 (2) and 1.5 (3) respectively with the fixed $V_2/V_a = 0.3$ where curve (2) corresponds to the boundary between the state I and the state II. The quantity $\partial^2 V(\theta, \pi/2)/\partial\theta^2$ at $\theta = \theta_0$, which denotes the second derivative of $V(\theta, \pi/2)$ with respect to θ at the ground state, is positive for curves (1) and (3) but becomes zero

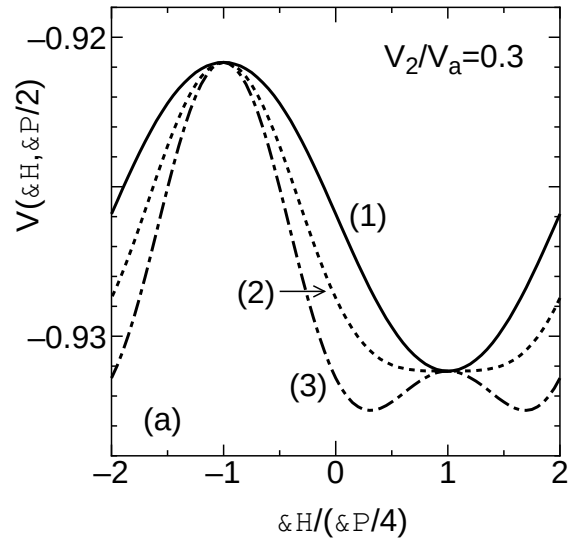

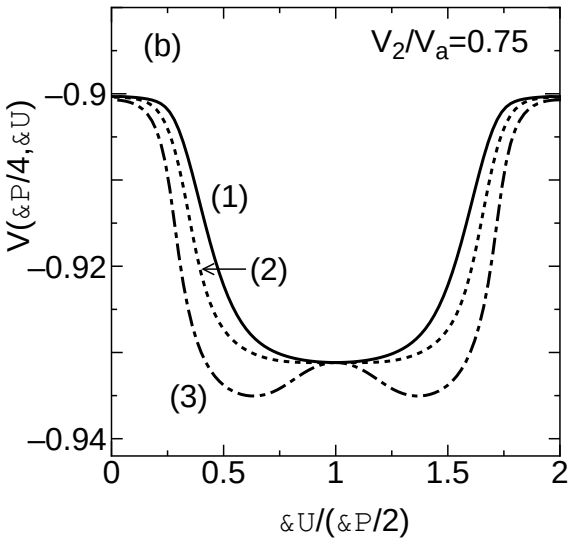

Fig. 6. (a) The θ-dependence of $V(\theta, \pi/2)$ for $V_a/t_b = 0.5$ (1), 1.13 (2) and 1.5 (3) with the fixed $V_2/V_a = 0.3$. (b) The ϕ-dependence of $V(\pi/4, \phi)$ for $V_a/t_b = 1.4$ (1), 1.66 (2) and 1.8 (3) with the fixed $V_2/V_a = 0.75$.

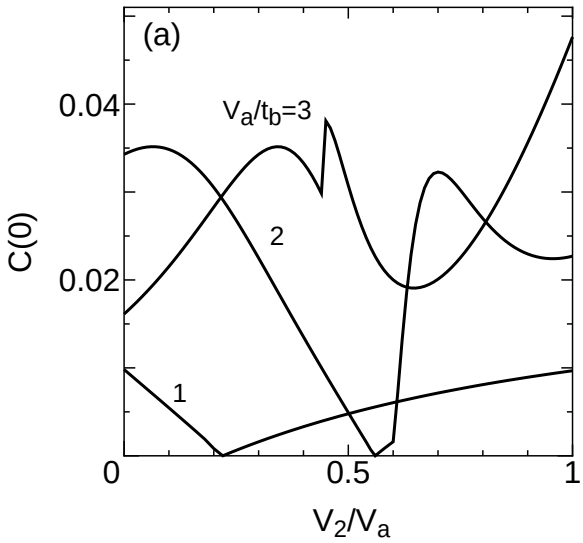

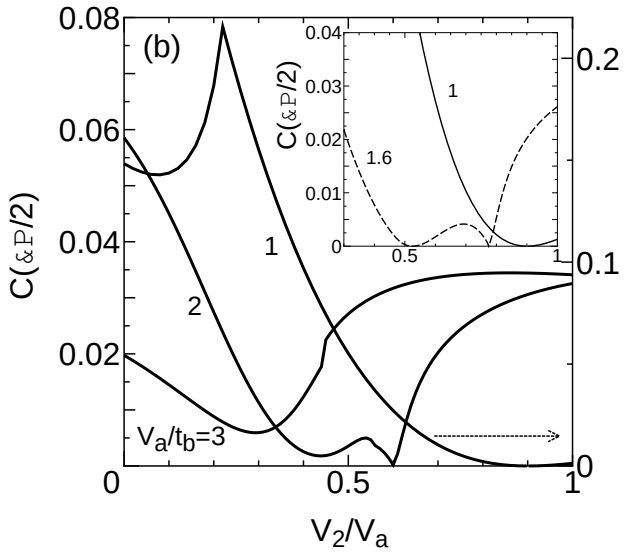

Fig. 7. (a)The V_2/V_a-dependence of $C(0)$ (eq. (2.15)) for $V_a/t_b = 1$, 2 and 3. (b)The V_2/V_a-dependence of $C(\pi/2)$ for $V_a/t_b = 1$, 2 and 3 where the right vertical axis is for $V_a/t_b = 1$. In the inset, the details of V_2/V_a-dependence of $C(\pi/2)$ is shown for $V_a/t_b = 1$ and 1.6.

for curve (2). Such a result has been already found for $V_2 = 0$ and $\delta V = 0$.[10] From Fig. 6(a), $V(\theta, \pi/2)$ can be written as $V(\theta, \pi/2) \simeq const. + W_c \cos 4\theta + W_d \sin 2\theta$, where W_c depends on both V_a and V_2 and W_d is mainly determined by $t_{\rm d}$. With increasing V_a (V_2), W_c decreases and becomes negative (increases and approaches to the limiting value with $V_a = 0$). In Fig. 6(b), the ϕ-dependence of $V(\pi/4, \phi)$ is shown for the three cases near the boundary of dotted curve of Fig. 4. Solid curve, dotted curve and dash-dotted curve are calculated for parameters with $(V_a/t_b, V_2/V_a) = (1.4, 0.75)$ (1), $(1.66, 0.75)$ (2) and $(1.8, 0.75)$ (3), which correspond to the state I, the boundary and the state III respectively. For curve (2), the second derivative of $V(\pi/4, \phi)$ with respect to ϕ becomes zero at $\phi = \pi/2$ while harmonic potential exists for curve (1) and (3). Thus it turns out that the harmonic potential with respect to ϕ vanishes only at the boundary between the state I and the state III.

It is of interest to examine how the harmonic potential for θ (ϕ) reduces to zero when parameters vary around the boundary given by the solid curve (the dotted curve) in Fig. 4. We calculate $C(\psi)$ given by eq. (2.15), which denotes a coefficient of harmonic potential with respect to θ and ϕ around θ_0 and ϕ_0, i.e., those of the ground state. Quantities $C(0)$ and $C(\pi/2)$ correspond to coefficients for θ and ϕ respectively. In Fig. 7(a), the V_2/V_a-dependence of $C(0)$ is shown for $V_a/t_b = 1$, 2 and 3 respectively. For $V_a/t_b = 1$, $C(0)$ becomes zero at $V_2/V_a = 0.22$, which corresponds to the boundary between the state I and the sate II. Such a behavior is similar to the V-dependence of the charge gap, which has been shown

for $V_2 = 0$.[10] For $V_a/t_b = 2$, $C(0)$ decreases to zero at $V_2/V_a = 0.56$, i.e., the boundary between the state I and the state II and exhibits a cusp at $V_2/V_a = 0.61$, i.e., the boundary between the state I and the state III. A shoulder is found in $C(0)$ for larger V_2/V_a. For $V_a/t_b = 3$, $C(0)$ exhibits a jump, at which a first order transition takes place due to the boundary between the state II and the state III. When V_2 increases further, $C(0)$ takes a minimum and increases rapidly. In Fig. 7(b), the V_2/V_a-dependence of $C(\pi/2)$ is shown for the same parameters as Fig. 7(a). For $V_a/t_b = 1$, $C(\pi/2)$ takes a cusp at $V_2/V_a = 0.22$ corresponding to a transition from the state II to the state I. With increasing V_2/V_a, $C(\pi/2)$ decreases rapidly and becomes zero at $V_2/V_a = 0.90$ where the quadratic behavior is seen around zero. The fact that such a zero value does not imply the boundary is explained at the end of this paragraph. For $V_a/t_b = 2$, $C(\pi/2)$ shows a small cusp at $V_2/V_a = 0.56$ corresponding to a transition from the state II to the state I. A zero of $C(\pi/2)$ at $V_2/V_a = 0.61$ comes from the boundary between the state I and the state III. For $V_a/t_b = 3$, $C(\pi/2)$ takes a jump at $V_2/V_a = 0.45$, which originates in the first order transition between the state II and the state III. In the inset, we show the detail behavior around the zero of $C(\pi/2)$ for $V_a/t_b = 1$ and 1.6. Quadratic behavior around the zero is seen for V_a/t_b=1. There are two kinds of zeros for $V_a/t_b = 1.6$ where the larger V_2 corresponds to the transition from the state I to the state III and exhibits a linear dependence around the zero. For $V_a/t_b = 1.6$, the quadratic behavior is also found around the smaller V_2, at which the actual transition does not occur. Such a fact is understood as follows. The effect of small variation of ϕ on the expectation value of eq.(2.11) is essentially determined by $\tilde{D}_{Q_0} \equiv N^{-1} \sum_{\sigma=\uparrow,\downarrow} \sum_{-\pi<k\leq\pi} \left\langle C^{\dagger}_{k\sigma} C_{k+Q_0,\sigma} \right\rangle$, where the average $<>$ is performed over eq.(2.4) with S_{mQ_0} and D_{mQ_0} replaced by trial fields, *e.g.*, $D_1 \propto \cos\phi$ and $S_1 \propto \sin\phi$. The ground state of the state I is the pure $2k_{\rm F}$-SDW with $\phi = \phi_0 = (\pi/2)$ and then quantities D_{Q_0} and $D^*_{Q_0}$ in the second line of eq. (2.4) vanishes due to $D_1 \propto \cos\phi$ and eq. (2.7b). When ϕ is varied from $\phi_0 = (\pi/2)$, the magnitude of D_{Q_0} and $D^*_{Q_0}$ becomes finite and the resultant $\tilde{D}_{Q_0}$ becomes finite generally. However there is a case where $\tilde{D}_{Q_0} = 0$ even for $D_{Q_0} \neq 0$ due to vanishing of the coefficient, *e.g.*, $U/2 - 2V_2 = 0$ for $\delta V = 0$. Such a case is examined explicitly in the next section. The location for $C(\pi/2) = 0$ corresponding to $\tilde{D}_{Q_0} = 0$ is shown by the thin dash-dotted curve in Fig. 4, where the vanishing of $C(\pi/2)$ exists only in the region I. The trajectory (thin dash-dotted curve) is nearly parallel to the dotted curve and crosses with the solid curve at $(V_a/t_b, V_2/V_a) \simeq (1.6, 0.5)$.

Further we examine $C(\psi)$ with arbitrary ψ, which induces the variation of both θ and ϕ. In Fig. 8, $C(\psi)$ is calculated for $(V_a/t_b, V_2/V_a)$= (0,0), (2,0), (2,0.6), (2,0.8) and (2,1), where $C(\psi + \pi/2) = C(\psi)$. The amplitude of $C(\psi)$ is large for $(0, 0)$ (shown by a vertical axis of right hand side) but becomes small in the presence of both V_a and V_2 as seen from (2, 0) and (2,1). The minimum of $C(\psi)$ is found at $\psi = 0$ for (0,0), (2,0) and (2,1) while it is found at $\psi = \pi/2$ for (2,0.6). Note that the minimum for (2,0.8) is located between $\psi = 0$ and $\psi = \pi/2$, where such a continuous variation of the minimum is seen for $0.80 < V_2/V_a < 0.86$ and $V_a/t_b = 2$ in the region III. The minimum of $C(\psi)$ at $\psi = \pi/2$ is obtained for parameters $(V_2/V_a, V_a/t_b)$ close to the dotted curve in Fig. 4. The quantity $C(\psi)$ exhibits a small ψ-dependence for (2,0.8). We comment on the behavior of $C(\psi)$ in Fig. 4. Within the numerical accuracy of the present calculation, we find $C(\psi) = 0$ at a critical point given by $(V_a/t_b, V_2/V_a) = (2.077, 0.576)$. The small magnitude of $C(\psi)$ shown for (2,0.6) is obtained for parameters of $(V_a/t_b, V_2/V_a)$, which are located near the critical point and also in the region enclosed by the dotted curve, solid curve and thin dash-dotted curve. Thus it is expected that the fluctuations for θ and ϕ become large around the solid curve and the dotted curve respectively and that the fluctuations for both θ and ϕ become large around the critical point of the intersection of these two curves .

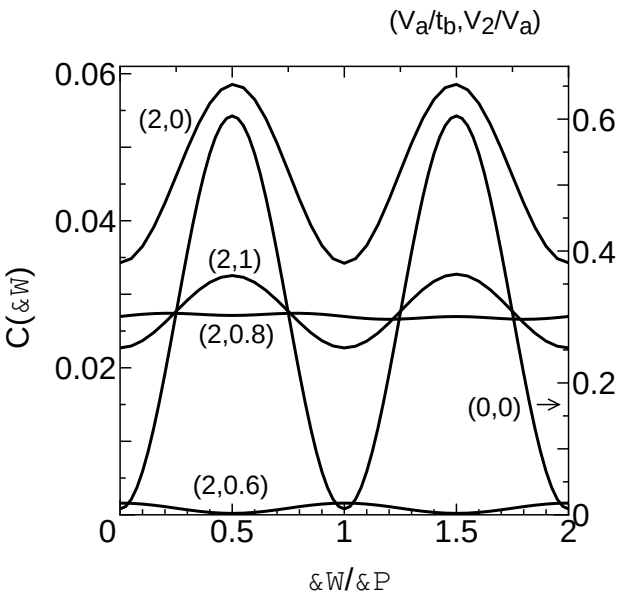

Fig. 8. The ψ-dependence of $C(\psi)$ for $(V_a/t_b, V_2/V_a)$= (0,0), (2,0), (2,0.6), (2,0.8) and (2,1). The right vertical axis is for (0,0).

Now we examine both θ and ϕ-dependences of $V(\theta, \phi)$ around the ground state by choosing parameters $(V_a/t_b, V_2/V_a)$= (0,0), (2,0), (2,0.6), (2,0.8) and (2,1), which are the same as Fig. 8. In Fig. 9, the θ-dependence of $V(\theta, \phi_0)$ is shown with the fixed $\phi = \phi_0$ where $\phi_0/\pi/2 = 1$ for (0,0), (2,0) and, (2,0.6) and $\phi_0/\pi/2 = 0.537$ and 0.499 for (2,0.8) and (2,1) respectively. There is a periodicity given by $V(\theta + \pi, \phi_0) = V(\theta, \phi_0)$. The θ-dependence of $V(\theta, \phi_0)$ is small for (0,0) and (2,0.6) (i.e., in the region I of Fig. 4) while it is large for (2,0), (2,0.8) and (2,1) (i.e., in the region of II and III of Fig. 4). The latter result comes from the fact that the variation of θ needs a large amount of energy due to the presence of the charge density of D_2 (D_1) in the region II (the region III).Figure 10 shows the corresponding ϕ-dependence for $V(\theta_0, \phi)$ where $\theta_0/(\pi/4) = 1$

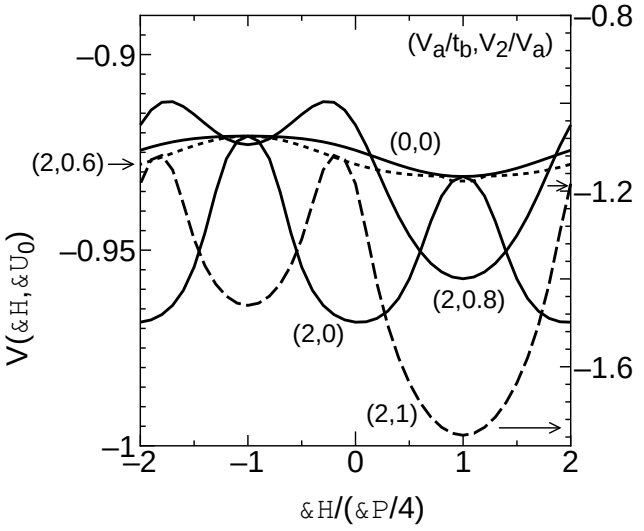

Fig. 9. The θ-dependence of $V(\theta, \phi_0)$ for $(V_a/t_b, V_2/V_a)$= (0,0), (2,0), (2,0.6), (2,0.8) and (2,1) where $\phi_0/\pi/2 = 1$ for (0,0), (2,0) and, (2,0.6) and $\phi_0/\pi/2 = 0.537$ and 0.499 for (2,0.8) and (2,1) respectively.

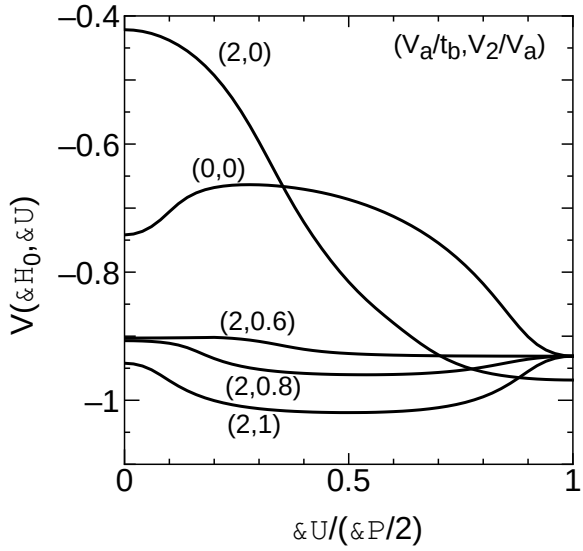

Fig. 10. The ϕ-dependence of $V(\theta_0, \phi)$ for $(V_a/t_b, V_2/V_a)$= (0,0), (2,0), (2,0.6), (2,0.8) and (2,1) where $\theta_0/\pi/4 = 1$ for (0,0), (2,0.6), (2,0.8) and (2,1) and $\theta/\pi/4 = 0.035$ for (2,0).

for (0,0), (2,0.6), (2,0.8) and (2,1) and $\theta/(\pi/4) = 0.035$ for (2,0) where $V(\theta_0, \phi) = V(\theta_0, \pi/2-\phi) = V(\theta_0, \phi+\pi)$. In the state III, ϕ_0 differs from $\pi/2$, which causes a small increase of $V(\theta_0, \phi)$ for the variation of ϕ. The variation of $V(\theta_0, \phi)$ is large for (2,0) and (0,0) and is small for (2,0.6), (2,0.8) and (2,1). This indicates a fact that the fluctuation of ϕ in the state I and II is small and that in the state III is large. The magnitudes of $V(\pi/4, \phi)$ for (0,0), (2,0.6), (2,0.8) and (2,1) becomes equal at $\phi = \pi/2$, since all these states reduce to the state I with the energy being independent of both V and V_2.

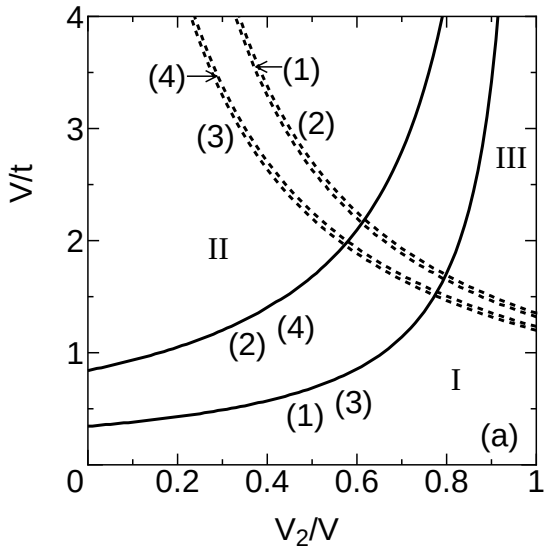

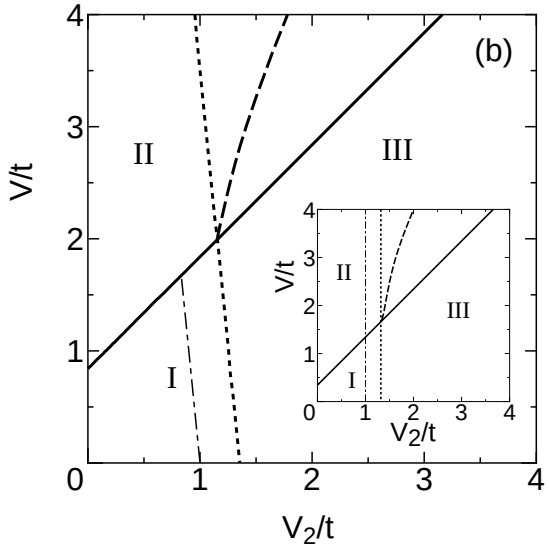

Fig. 11. (a)Phase diagram on the plane of V_2/V and V/t where the solid curve (the dotted curve) denotes the boundary between the state I and the state II (the state I and the state III). Parameters are taken as $(t_d/t, \delta V/V)$ = (0,0) (1), (0.1,0) (2), (0,0.1) (3), (0.1,0.1) (4). (b)Phase diagram on the plane of V_2/t and V/t where $U/t = 4$ and $(t_d/t, \delta V/V)$ = (0.1,0.1). The notation of curves are the same as Fig. 4. In the inset, another phase diagram is shown for $U/t = 4$ and $(t_d, \delta V)$ = (0,0).

§4. Discussion

In the present paper, we have examined several kinds of SDW states in a one-dimensional quarter-filled electron system with long range Coulomb interaction within the mean-field theory. The phase diagram of the SDW state with the states I, II and III were obtained on the plane of V_2/V_a and V_a/t_b. The variation of the energy from that of the ground state was calculated in order to examine the role of phase variables of the SDW states.

Here we examine the effect of δV and t_d on the boundaries in the phase diagram of Fig. 4. In Fig. 11(a), the several results of boundaries are shown where the solid

curve (the dotted curve) denote the boundary between the state I and the state II (the state I and the state III). Parameters are taken as $(t_{\rm d}/t, \delta V/V)$ = (0,0) (1), (0.1,0) (2), (0,0.1) (3), (0.1,0.1) (4) where curve (4) corresponds to Fig. 4. Since solid curve (2) (solid curve (1)) is the the same as solid curve (4) (solid curve (3)), the boundary between the state I and the state II depends on $t_{\rm d}$ but does not depend on δV. The energy gain by the formation of $4k_{\rm F}$-CDW decreases by the dimerization but not by the alternation of nearest-neighbor interaction. From the dotted curves where curves (3) and (4) are located below curves (1) and (2), it is found that the energy gain by the formation of $2k_{\rm F}$-CDW is increased by δV. The dotted curve moves slightly upward in the presence of $t_{\rm d}$. We note that the comparison of solid curve (4) and solid curve (3) (dotted curve (4) and dotted curve (2)) demonstrates explicitly the argument by Kobayashi et *al.*[11] that the region II is enlarged by in the absence of $t_{\rm d}$ (and that δV increases the region III).

In order to understand the coexistent state clearly, another phase diagram is calculated on the plane of V_2/t and V/t where $V = (V_a + V_b)/2$ and $t = (t_a + t_b)/2$. by choosing another parameters for both axes. In Fig. 11(b), a phase diagram corresponding to Fig. 4 is shown with $U/t = 4$ and $(t_{\rm d}/t, \delta V/V)$ = (0.1,0.1). The point, which shows the intersection of the solid curve and the dotted curve, is given by $(V_2/t, V/t)$=(1.15,2.0). We find, within the numerical accuracy, that the boundary between the state I and II (the solid curve) is expressed as $V = V_2 + const.$. Such a V_2-dependence is understood from the coefficient of D_{2Q_0} in eq. (2.4), i.e., $(U/2 - 2V + 2V_2)$. The quantity, V, which is needed to create $4k_{\rm F}$-CDW, is replaced by $V - V_2$ for $V_2 \neq 0$. The dotted curve denotes a critical value of V_2/t, above which the $2k_{\rm F}$-CDW appears. The tangent of the dotted curve depends on δV. In the inset, a phase diagram is shown for $U/t = 4$ and $(t_{\rm d}, \delta V) = (0,0)$. The dotted curve becomes straight due to $\delta V = 0$, since the boundary between the state I and the state III are determined only by V_2/t in the absence of $t_{\rm d}$ and δV. It turns out that the $2k_{\rm F}$-CDW is induced by the next-nearest-neighbor interaction but not by the nearest-neighbor interaction. The second term of eq. (2.4) shows that the coefficients, $(U/2 - 2V_2)$, of D_{Q_0} changes the sign at $V_2/t = 1$ for $U/t = 4$ and that the $2k_{\rm F}$-CDW is induced for larger V_2/t *e.g.*, $D_1 \neq 0$ for $V_2/t \gtrsim 1.3$. Further we comment on the condition for $C(\pi/2) = 0$, which occurs on the thin dash-dotted curve in Figs. 4 and Fig. 11(b). The inset of Fig. 11(b) displaying $C(\pi/2) = 0$ at $V_2 = U/4$, is interpreted from the fact that the coefficient of D_{Q_0} in the second line of eq. (2.4) becomes zero at $V_2 = U/4$ resulting in the zero value of $2k_{\rm F}$-CDW.

Finally we discuss the experimental results based on our result. In the present calculation, the state, which exhibits the coexistence of the $2k_{\rm F}$-SDW and $2k_{\rm F}$-CDW[11] followed by $4k_{\rm F}$-SDW, has been obtained for a model with the on site, nearest-neighbor and next-nearest-neighbor interactions, i.e., the purely electronic interactions. The experimental results of the coexistence of $2k_{\rm F}$-SDW and $2k_{\rm F}$-CDW in TMTSF-salts[7] seems to be consistent with the calculation. However the experiment indicates also the $4k_{\rm F}$-CDW, which is absent in the present calculation. Such a discrepancy between the experiment and the theory may suggest a role of the electron-phonon interaction, which gives rise to the density wave in addition to the purely electronic interaction. Further, it will be an interesting problem to elucidate if $4k_{\rm F}$-SDW obtained in the present calculation is observed in the coexistent state of the Bechgaard salts.

Acknowledgment

This work was partially supported by a Grant-in-Aid for Scientific Research from the Ministry of Education, Science, Sports and Culture (Grant No.09640429).

[1] D. Jérome and H. J. Schulz: Adv. Phys. **31** (1982) 299.
[2] T. Ishiguro and K. Yamaji: *Organic Superconductors*(Springer Verlag, 1990).
[3] J. M. Delrieu, M. Roger, Z. Toffano, E. Wope Mbougue, P. Fauvel, R. Saint James and K. Bechgaard: Physica. **143B** (1986) 412; J. M. Delrieu, M. Roger, Z. Toffano, A. Moradpour and K. Bechgaard: J. Phys. France **47** (1986) 839.
[4] T. Takahashi, Y. Maniwa, H. Kawamura and G. Saito: J. Phys. Soc. Jpn. **55** (1986) 1364; Physica **143B** (1986) 417.
[5] K. Penc and F. Mila: J. Phys. I (France) **3** (1993) 155; Phys. Rev. B **50** (1994) 11429; F. Mila: Phys. Rev. B **52** (1995) 4788.
[6] G. Grüner: Rev. Mod. Phys. **66** (1994) 1.
[7] J. P. Pouget and S. Ravy: J. Phys. I (France) **6** (1996) 1501; Synth. Metals **85** (1997) 1523.
[8] S. Kagoshima, Y. Saso, M. Maesato, R. Kondo and T. Hasegawa: Solid State Commun. **110** (1999) 479.
[9] H. Seo and H. Fukuyama: J. Phys. Soc. Jpn. **66** (1997) 1249.
[10] Y. Suzumura: J. Phys. Soc. Jpn. **66** (1997) 3244.
[11] N. Kobayashi, M. Ogata and K. Yonemitsu: J. Phys. Soc. Jpn. **67** (1998) 1098.
[12] A.W. Overhauser: Phys. Rev. **167** (1968) 691.
[13] P. A. Lee, T. M. Rice and P. W. Anderson: Solid State Commun. **14** (1974) 703.
[14] S. Takada: J. Phys. Soc. Jpn. **53** (1984) 2193.
[15] A. Virosztek and K. Maki: Phys. Rev. B **37** (1988) 2028; K. Maki and A. Virosztek: Phys. Rev. B **41** (1990) 557.
[16] Y. Suzumura: J. Phys. Soc. Jpn. **59** (1990) 1711.
[17] Y. Suzumura and N. Tanemura: J. Phys. Soc. Jpn. **64** (1995) 2298.